Tianjin Daxue Xuebao (Ziran Kexue yu Gongcheng Jishu Ban)/
Journal of Tianjin University Science and Technology
ISSN (Online):0493-2137
E-Publication: Online Open Access
Vol: 57 Issue: 12:2024
DOI: 10.5281/zenodo.16525521

DESIGN OF A MINIATURIZED CONICAL SURFACE HIGH ISOLATION MULTICHANNEL ANTENNA FOR MISSILE GUIDANCE APPLICATIONS

SEKHAR BABU KURMA
Assistant Professor, DNR College of Engineering & Technology Bhimavaram A.P, India.
Email: sekharciet@gmail.com

VENUGOPAL KONDAPALLI
Associate Professor, DNR College of Engineering & Technology Bhimavaram A.P, India.
Email: venugopal.kondapalli@gmail.com

B. KIRAN BABU
Associate Professor, Godavari Global University Rajahmundry, A.P. India.
Email: bkiranbabu87@gmail.com

MARY LEENA NALLAGANGULA
Assistant Professor, DNR College of Engineering & Technology Bhimavaram A.P, India.
Email: leenaprasad414@gmail.com

VENKAT RAO NEKKANTI
Professor, DNR College of Engineering & Technology Bhimavaram A.P, India.
Email: venkatraonekkanti@gmail.com

G. RANGARAO
Lecturer, DNR College Bhimavaram A.P, India. Email: rangraogolla1975@gmail.com

Abstract

This paper introduces a novel four-port multiple-input multiple-output antenna constructed with a conical surface geometry that surmounts the constraints of prior models intended for ultrawide-band applications, such as missile guidance applications. Each orthogonal element spans a stepped rectangular patch fed by a tapered microstrip line, offering polarization diversity. This structure shrinks the dimensions of the antenna to 42 × 42 mm2. A minuscule pair of non-driven elements on the rear Reflective surface functions as a decoupling element Mediating adjoining ports to further boost functionality. Curiously designed in the shape of a windmill and spinning cross, the tapes elevate the isolation. The proposed dual-band monopole antenna was designed on a compact FR4 substrate with a permittivity of 4.4 and a thickness of only 1 mm. Measurements revealed an impressive impedance bandwidth from 3.5 GHz to well beyond 16 GHz along with isolation exceeding 20 dB between the two ports. The envelope correlation was a negligible 0.0002 while diversity gain reached a hearty 10 dB across the band. Group delay differed by less than 1 ns throughout. Though other designs may perform better regarding one or two of these metrics, our antenna achieves a deft equilibrium of bandwidth, size, and isolation unlike anything yet reported. While demonstrating quite pleasing quasi-omnidirectional radiation over its broad operational range, making it well-suited for an array of emerging wireless applications, notably in minimized gadgets, a more nuanced evaluation of its design is still warranted to realize its potential for the networks of the future fully.

Index Terms: Ultra-Wideband Antenna, Diversity Gain, Mean Effective Gain, Group Delay, Multi-Input Multi. Return Loss, ECC.

Tianjin Daxue Xuebao (Ziran Kexue yu Gongcheng Jishu Ban)/
Journal of Tianjin University Science and Technology
ISSN (Online):0493-2137
E-Publication: Online Open Access
Vol: 57 Issue: 12:2024
DOI: 10.5281/zenodo.16525521

1. INTRODUCTION

This document Modern missile systems rely upon intricate radar guidance apparatuses to accurately target and intercept their intended objectives. These radars function by emitting electromagnetic waves and dissecting the echoed signals to determine the location, velocity, and trajectory of the objective. A missile guidance radar's frequency can fluctuate depending on its structure and purpose. However, some frequent wavelength bands employed for missile guidance radars include: The C-band, ranging from 4 to 8 GHz, which is commonly utilized for long-range missile guidance radars. It offers a suitable balance between range and definition. This band allows radars to detect targets from afar while maintaining enough resolution to track swift aerial maneuvering. The X-band, ranging from 8 to 12 GHz, is often implemented for shorter-range missile guidance radars. It furnishes enhanced definition but has a more confined range compared to the C- band. This higher frequency provides clarity on nearer targets but signals weaken over longer distances, restricting its usage to close-quarters interceptions.

The tremendous growth and rapid development in the field of wireless communication have motivated researchers to explore groundbreaking technologies that can enable unprecedented data transmission speeds.[4] Ultrawideband (UWB) technology has attracted considerable interest owing to its exceptionally expansive bandwidth, phenomenally superior data rates, and remarkable resilience against disruption. Since the Federal Communications Commission (FCC) opened up the 3.1–10.6 GHz spectrum for unlicensed commercial applications, UWB has emerged as a revolutionary wireless protocol with diverse communications, radar, wearable gadgets, and medical innovation applications. However, the comparatively low transmission power of UWB systems restricts their working distances.[3] Yet combining UWB with multiple-input multiple-output (MIMO) strategies has proven highly effective in bolstering immunity against multipath interference effects. By capitalizing on multiple transmit and receive antennas, MIMO amplifies the transmission rate of wireless networks, substantially persisting the operating range of UWB systems.[2] For UWB-MIMO antenna research, broad bandwidth and high isolation remain fundamental objectives. Developing UWB-MIMO antennas poses the challenge of mitigating coupling between antenna elements within compact form factors with constrained space. [6] To satisfy isolation needs, the spacing between antenna units must reach half the minimum wavelength in the UWB band—yielding overwhelmingly large antenna dimensions.[5] Thus, appropriate decoupling geometries between radiating components aim to boost isolation. Diverse decoupling schemes have been tried for MIMO antennas. Some designs attain good isolation via orthogonal polarization and optimized element placement without extra structures. Others mitigate mutual coupling by symmetric layouts and separating four-directional staircases.[8] Some incorporate perpendicular microstrip feeds plus parasitic strips between adjacent feeds. Periodic linear networks of square-ring resonators or ground stubs often yield strong isolation using electromagnetic bandgap columns.[9] However, effectively balancing the antenna size, isolation ambiguity, and cost remains challenging across all proposed designs. While some methods can enrich isolation by utilizing fragmentation diversity, their large proportions preclude useful integration.[11] Others meet the necessary UWB

Tianjin Daxue Xuebao (Ziran Kexue yu Gongcheng Jishu Ban)/
Journal of Tianjin University Science and Technology
ISSN (Online):0493-2137
E-Publication: Online Open Access
Vol: 57 Issue: 12:2024
DOI: 10.5281/zenodo.16525521

specifications but achieve only suboptimal isolation. Both complex fabrication processes and difficult tuning tend to hinder certain antenna configurations.[1] In contrast, using expensive high-frequency substrates makes possible small sizes and high isolation yet increases expenses. This paper presents a low-cost, compact, high-isolation, four-port UWB-MIMO antenna well-suited for ultra-broadband networks.[15] The identically configured orthogonal antenna elements minimize the overall footprint. Individually, each antenna patch contains both a stepped rectangular shape and an asymptote-like feed structure optimized to broaden the operational bandwidth. Backside windmills and rotating crosses reduce coupling between radiators. Simulations and measurements validate the wideband, highly isolated performance, radiation, diversity, and peak gain characteristics. Key contributions include a stepped patch layout, orthogonal configuration, asymptote feed, and windmill/cross decouplers—all combining to maximize bandwidth, isolation, and size efficiency at low cost.[21]

2. DESIGN METHODOLOGY OF CONICAL-SHAPED MIMO ANTENNA

The engineer began with a straightforward microstrip antenna comprised of a flat rectangular conducting patch situated above a ground plane using a narrow strip to deliver radio signals.[1] Initial assessments found it effectively received between 4.07 and 8.05 gigahertz, a workable if limited ambit. Seeking to expand the scope of frequencies, modifications were devised and tested. At the outset, small voids were carved out from the lower edge of the patch, lengthening the current route and bringing new resonance points, pushing performance to 3.83 to 5.19 gigahertz and 6.97 to 10.5 gigahertz. [30]Yet even with progress, more was still required to encompass the desired ultra-wide domain. Next, notches were cut into the strip itself, morphing its even form into an irregular shape. This revision performed well, achieving under 10-decibel return loss from 3.5 to 13 gigahertz. As a concluding refinement, the underlying ground plane was indented too, widening the span even further to a broad 3.5 to 16 gigahertz. Through iterative adjustments, the assortment of supported frequencies was astonishingly expanded. The fundamental parts of a rectangular microstrip antenna include the substrate, patch, ground plane, and delivery strip. To get initial sizes for the patch operating at a specified frequency, elementary calculations using basic equations can supply apt starting values. Plugging the relative permittivity, velocity of light, and operating frequency into Equations 1 and 2 yields provisional length and width for the patch. Selecting an optimum width using this length aims for good impedance matching. The primary calculations were as follows:

$$w - \frac{C}{2F}\left(\frac{\Sigma r+1}{2}\right)^{-\frac{1}{2}} \quad (1)$$

$$L = \lambda_e = 2\Delta L \quad (2)$$

$$\lambda e = \frac{C}{f\sqrt{\Sigma e}} \quad (3)$$

$$\text{Length of feed line} = \frac{\lambda}{4\sqrt{\Sigma r}} \quad (4)$$

The effective dielectric constant (ε_{reff})

$$\varepsilon_{reff} - \frac{\varepsilon+1}{2} + \frac{\varepsilon-1}{2}\left[\frac{h}{w_p}\right]^{-\frac{1}{2}} \quad (5)$$

Tianjin Daxue Xuebao (Ziran Kexue yu Gongcheng Jishu Ban)/
Journal of Tianjin University Science and Technology
ISSN (Online):0493-2137
E-Publication: Online Open Access
Vol: 57 Issue: 12:2024
DOI: 10.5281/zenodo.16525521

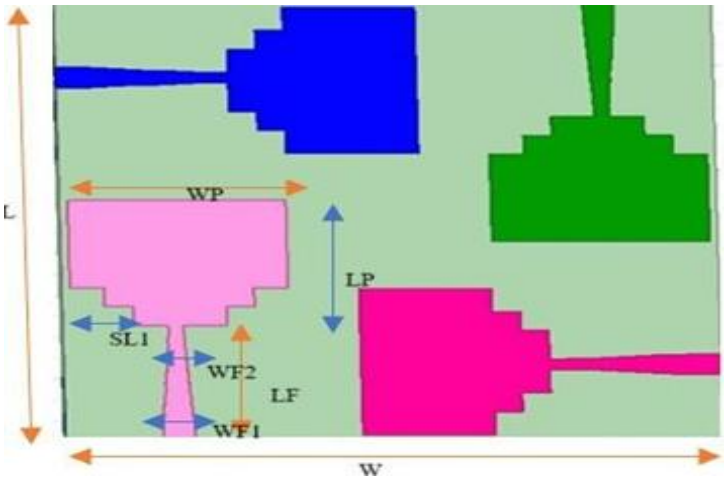

Figure 1: Emitting component of mimo antenna

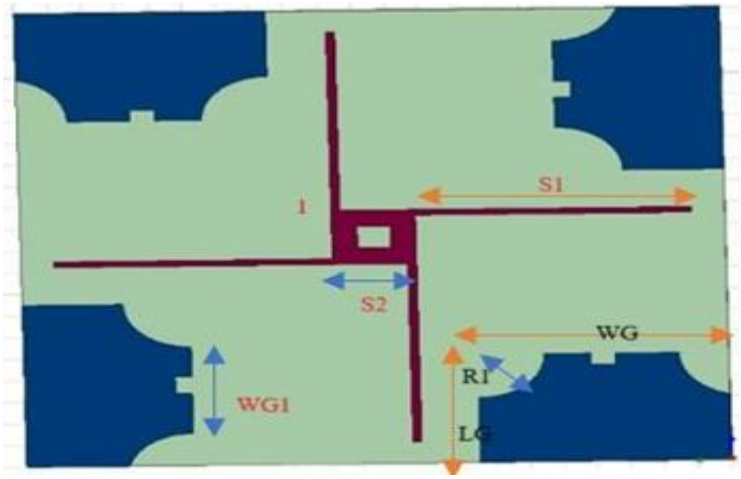

Figure 2: Earth surface of the mimo antenna

Table 1: Antenna dimensions (Optimized).

Parameter of the Design	Dimension (mm)	Parameter of the Design	Dimension (mm)	Parameter of the Design	Dimension (mm)	Parameter of the Design	Dimension (mm)
W	22	LF	11	LG	10	S1	18
L	22	WF1	2	WG	15	S2	4
WP	14	WF2	1	R1	2	WG1	11
LP	12	SL1	4.5				

3. RESULTS AND DISCUSSION

While antenna design considerations span myriad factors, several elements notably impact performance. This paper explores properties central to efficiency, examining the radiating components through simulation results. A high-frequency structure simulator utilizing optimization techniques modeled the antenna element. A variety of parameters

Tianjin Daxue Xuebao (Ziran Kexue yu Gongcheng Jishu Ban)/
Journal of Tianjin University Science and Technology
ISSN (Online):0493-2137
E-Publication: Online Open Access
Vol: 57 Issue: 12:2024
DOI: 10.5281/zenodo.16525521

were experimented with, from the positioning of feeds informing directivity to material selections affecting signal propagation. Radiation patterns arose from intriguing interactions as element designs were tweaked. A deeper understanding of an antenna's operation emerged from studying the complex interplay between its distinctive structural characteristics.

3.1 Return Loss

Return loss plays a pivotal role in showcasing the operating range of the proposed antenna design. Systems with high return loss are more effective than those with low return loss, as more of the emitted power reaches the intended recipient rather than reflecting backward.[28] As Figure 3 illustrates, the proposed antenna's scattering parameters—more commonly known as return loss—were simulated at -45dB at 4.9GHz and -42dB at 12GHz, respectively demonstrating desirable transmission qualities within those bands. The non- uniform reflection properties across frequencies lend meaningful insight into the antenna's capacity for transmitting signals across a varied range, with less wasted energy returned to the sender.

$$RL\ dB=10\log\ Pi/Pr \qquad (6)$$

3.2 Voltage Standing Wave Ratio

The ratio of maximum and minimum voltage levels on a transmission line dictates its voltage standing wave ratio. Ideally, VSWR should be as close to 1 to minimize reflections and ensure quality signal transmission without distortion.[24] However, a perfectly matched line is difficult to engineer given variations in component characteristics and environmental factors. The graph depicted two VSWR curves derived through theoretical modeling and experimental measurement of a radiating element. It allows evaluation of how closely the constructed prototype matches the intended design. While a low VSWR <2 is preferable, well above 3 can induce perceptible degradation and should be avoided, when possible, through impedance matching techniques. To transfer information without corrupting its fidelity, transmission system engineers aim to tame impedance irregularities that give rise to elevated voltage ratios along the distributed line. [30]

$$VSWR=Vmax/Vmin \qquad (7)$$

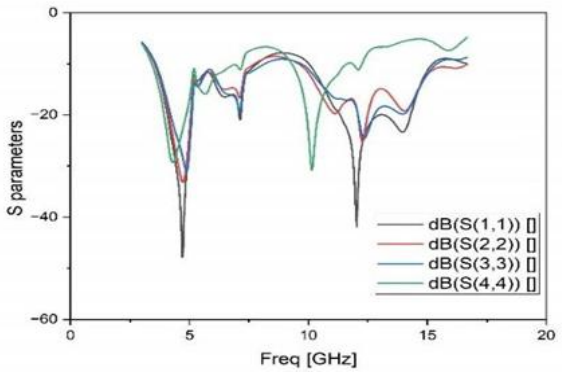

Figure 1: Return Loss curve

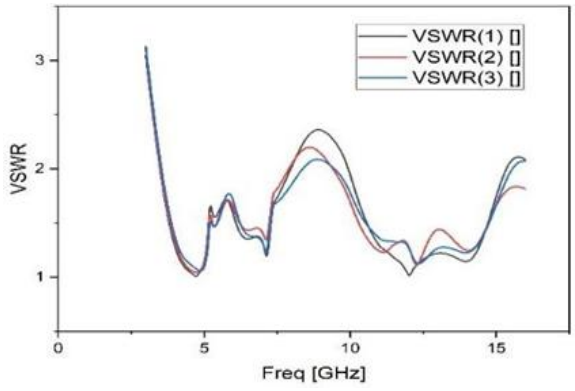

Figure 4: VSWR curve

Tianjin Daxue Xuebao (Ziran Kexue yu Gongcheng Jishu Ban)/
Journal of Tianjin University Science and Technology
ISSN (Online):0493-2137
E-Publication: Online Open Access
Vol: 57 Issue: 12:2024
DOI: 10.5281/zenodo.16525521

3.3 Antenna Gain

Antenna gain is the highest efficiency with which an antenna can radiate the power produced by the transmitter in the direction of a target.[12] Usually, antenna gain is denoted by the letter G. Figure .5(a) depicts the modeled gain for the proposed antenna. Figure 5(b) depicts the radiation diagram for the Intended antenna at 8GHz.with a gain of 6dBi

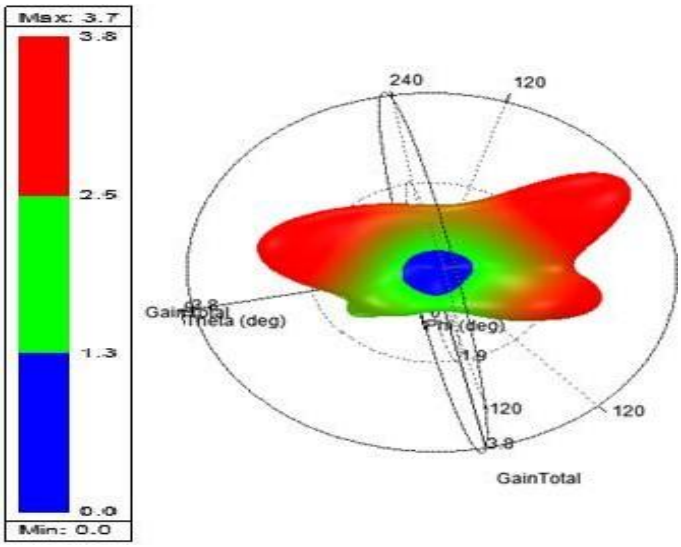

Figure 5: (a) Antenna gain polar plot at 8 GHz

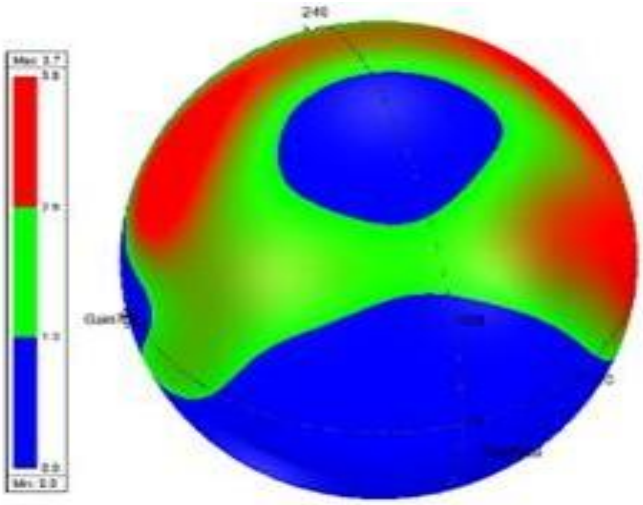

Figure 5: (b) Antenna gain spherical plot plot at 8 GHz

3.4 Group Delay

Group delay, a complex temporal characteristic inherent to multi-input multi-output antennas, influences the transmitted signals as data permeates a linear system. This metric, otherwise known as envelope delay, portrays the propagation timing of the

Tianjin Daxue Xuebao (Ziran Kexue yu Gongcheng Jishu Ban)/
Journal of Tianjin University Science and Technology
ISSN (Online):0493-2137
E-Publication: Online Open Access
Vol: 57 Issue: 12:2024
DOI: 10.5281/zenodo.16525521

combined waveform.[1] Therefore, figure 6 demonstrates the fluctuations in the group delay within the operating scope of the proposed MIMO layout. Particularly, the group delay from the primary port to itself (1,1) represents the delay, whereas the group delay from the primary port to the second port (1,2) portrays the time. The group delays from the primary port to the third (1,3) and fourth ports (1,4) follow a similar pattern. Interestingly, aberrations were magnified at higher frequencies as frequencies exacerbated the distortions. The total group delay of the proposed antenna configuration was under one nanosecond, maintaining a minimal delay.

3.5 Envelop Correlation Coefficient(ECC)

While mutual coupling presents a notable challenge for MIMO antennas seeking to maximize throughput, innovative design approaches continue pushing the boundaries of radiative performance.[10] State-of-the-art models anticipate cross-correlation values below half a percentage point across applicable wavelengths. As depicted in the diagram, physical validation of an ultra-compact multifunctional array corroborates exceptionally low eccentricity compensation coefficients ranging from zero to two thousandths throughout the bandwidth, thereby fulfilling expectations for radiative adequacy wherever spectral realms demand reliable interconnectivity.[1] Nevertheless, as transmission densities increase, mutual interference will likely necessitate more sophisticated solutions to optimize the concurrent usability of closely packed radiators while upholding resilience against distortion.

$$ECC = \frac{|S11*S12+S21*S22|^2}{(1-|S11|^2-|S21|^2)(1-|S22|^2-|S12|^2)} \quad (8)$$

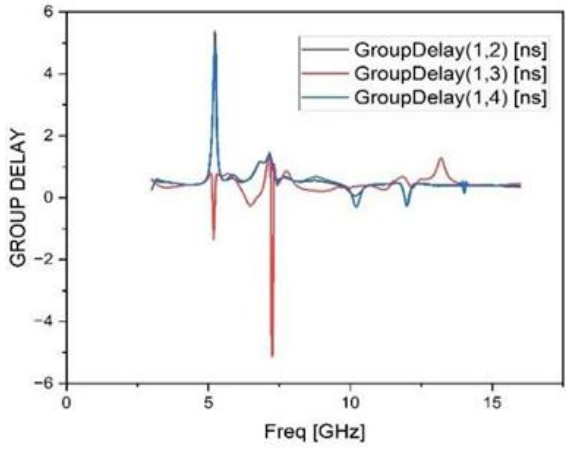

Figure 6: Group delay of mimo antenna

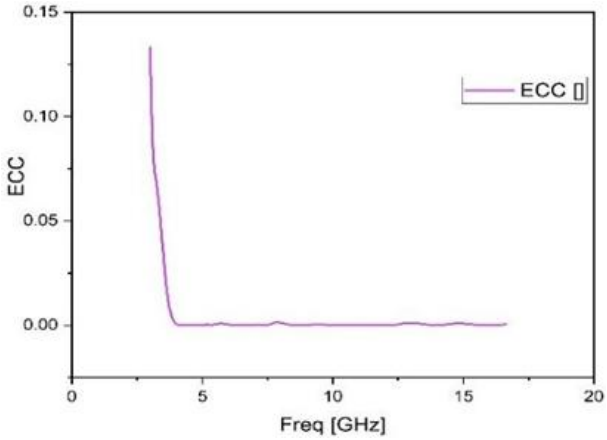

Figure 7: ECC curve of mimo antenna

3.6 Diversity Gain

When the signals first reached the receivers, the diversity gain was immediately set to work analyzing and comparing the signals' strength and clarity across the various frequencies.[25] Equation 9 smoothly illustrates the quantifiable increases in signal-to-

Tianjin Daxue Xuebao (Ziran Kexue yu Gongcheng Jishu Ban)/
Journal of Tianjin University Science and Technology
ISSN (Online):0493-2137
E-Publication: Online Open Access
Vol: 57 Issue: 12:2024
DOI: 10.5281/zenodo.16525521

noise ratio resulting from the divergence gain's complex calculations at each moment. As Figure 9 vividly portrays, the techniques steadily boosted the ratio along the full ultra-wideband, peaking impressively above 9.99 dB at certain points. Through artfully mitigating the fluctuating ravages of fading and moderating its intermittent corrupting consequences, which have long troubled wireless communication's reliability, the system demonstrated its power to both elevate signal quality and fortify it through diversity and an antenna cluster's combined insights.[20]

$$DG = 10\sqrt{1 - (ECC)2} \qquad (9)$$

3.7 Mean Effective Gain

MEG, a pivotal measure for evaluating diversity effectiveness, symbolizes the typical vitality Collected by a diversity receiver in an intricate multipath failing experience likened to the intensity accrued by a non-directional receiver.[28] Greater MEG beliefs in wireless interaction schemes can enable additional elevated transmission rates, which are imperative for massive information programs similar to intensive information ones or moving graphic exchanges. Moreover, systems with a higher MEG can sustain connection realize augmented dependability, and decrease the possibility of transmission failing even in changing channel circumstances.[31] At the same time, receivers with optimized MEG values have the aptitude to augment the usefulness and high quality of providers for end users.[14]

MEG1=0.5[1-|S11|2-|S12|2] (10)

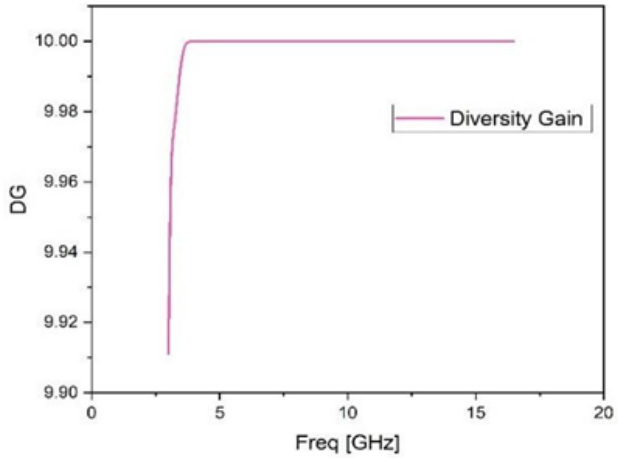

Figure 8: DG curve of mimo antenna

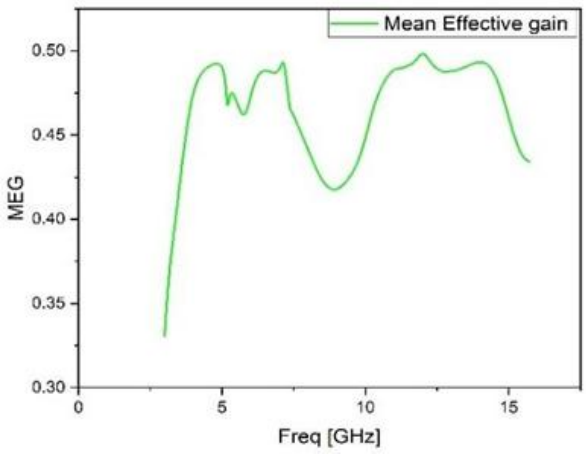

Figure 9: MEG curve of mimo antenna

Tianjin Daxue Xuebao (Ziran Kexue yu Gongcheng Jishu Ban)/
Journal of Tianjin University Science and Technology
ISSN (Online):0493-2137
E-Publication: Online Open Access
Vol: 57 Issue: 12:2024
DOI: 10.5281/zenodo.16525521

Table 2: Comparison of Proposed antenna against the references

Ref.	Band Width (GHz)	Size (mm) & Material	Gain dBi	Isolation	ECC
8	3-15	38*38*0.7625 Neltec	0.5-5	>15	<0.5
10	3-11	60*60*1.6 FR4	>3.4	>20	<0.02
25	3-13.5	58*58*0.8 FR4	2.2-4	>22	<0.008
26	3.2-14	16*71.5*0.254 RT Duriod 5880	3-5.6	>22	<0.006
27	3-13.2	38.3*38.3*0.8 Taconic	0.6-6.3	>17	<0.003
28	3.1-10.6	50*50*1.6 FR4	2-6	>17	<0.002
29	3.89-17.9	56.1*67.9*2.3 FR4	3.4-6.8	>15	<0.002
30	3-11	42*42*1.6 FR4	3-4.5	>15	<0.005
1	3.09-12	42*42*1 FR4	2-5.1	>16	<0.002
Prop.	3.5-16	42*42*1 FR4	>6.2	>20	<0.0002

4. CONCLUSION

This paper proposes a compact four-element UWB-MIMO antenna system with useful characteristics. The antenna model incorporated strangely shaped structures in the transmitting patch, microstrip feed network, and isolation design to achieve a small-sized yet impressive bandwidth range. Remarkably, the outcomes were aligned with the predicted results. Most significantly, the antenna functioned across the immense frequency range of 3.5-15 GHz while maintaining an overall area of just 42 by 42 mm, less than half the wavelength at the bottom frequency. Moreover, it realized isolation below -20 dB, confirming its extremely compact nature and noteworthy signal separation ability. The radiation and MIMO spatial diversity qualities were also quite satisfactory, with an ECC under 0.00002, a DG greater than 9.991 dB consistently throughout the wide operational band, and a group delay uniformly under 1 ns across the expansive passband. The antenna demonstrated well-matched S-parameters and a good correlation between the predicted and measured results, verifying its efficacy for numerous MIMO applications demanding reduced size and elevated performance.

References

1) Wu, A.; Tao, Y.; Zhang, P.; Zhang, Z.; Fang, Z. A Compact High-Isolation Four-Element MIMO Antenna with Asymptote-Shaped Structure. Sensors 2023, 23, 2484.

2) Powell, J.; Chandrakasan, A. Differential and single-ended elliptical antennas for 3.1–10.6 GHz ultrawideband communication. In Proceedings of the Antennas and Propagation Society International Symposium, Sendai, Japan, 20–25 June 2004; pp. 2935–2938.

3) El-Hameed, A.S.A.; Wahab, M.G.; Elshafey, N.A.; Elpeltagy, M.S. Quad-port UWB MIMO antenna based on LPF with vast rejection band. AEU-Int. J. Electron. Commun. 2021, 134, 153712. [CrossRef]

4) Manoharan, H.; Selvarajan, S.; Yafoz, A.; Alterazi, H.A.; Chen, C. Deep Conviction Systems for Biomedical Applications Using Intuiting Procedures with Cross Point Approach. Front. Public Health 2022, 10, 909628.

5) Iqbal, A.; Smida, A.; Alazemi, A.J.; Waly, M.I.; Mallat, N.K.; Kim, S. Wideband Circularly Polarized MIMO Antenna for High Data Wearable Biotelemetric Devices. IEEE Access 2020, 8, 17935–17944.

Tianjin Daxue Xuebao (Ziran Kexue yu Gongcheng Jishu Ban)/
Journal of Tianjin University Science and Technology
ISSN (Online):0493-2137
E-Publication: Online Open Access
Vol: 57 Issue: 12:2024
DOI: 10.5281/zenodo.16525521

6) Ibrahim, A.A.; Abdalla, M.A.; Abdel-Rahman, A.B.; Hamed, H.F. Compact MIMO Antenna with Optimized Mutual Coupling Reduction Using DGS. Int. J. Microw. Wirel. Technol. 2014, 6, 173–180.

7) Toktas, A.; Akdagli, A. Compact multiple-input multiple-output antenna with low correlation for ultra-wide-band applications. IET Microw. Antennas Propag. 2015, 9, 822–829.

8) Sipal, D.; Abegaonkar, M.P.; Koul, S.K. Easily Extendable Compact Planar UWB MIMO Antenna Array. IEEE Antennas Wirel. Propag. Lett. 2017, 16, 2328– 2331.

9) Khan, M.S.; Capobianco, A.D.; Asif, S.; Iftikhar, A.; Braaten, B.D. A 4-element compact Ultra-Wideband MIMO antenna array. In Proceedings of the IEEE International Symposium on Antennas & Propagation & USNC/URSI National Radio Science Meeting, Vancouver, BC, Canada, 19–24 July 2015.

10) Ahmad, S.; Khan, S.; Manzoor, B.; Soruri, M.; Alibakhshikenari, M.; Dalarsson, M.; Falcone, F. A Compact CPW-Fed Ultra WidebandMulti-Input-Multi-Output (MIMO) Antenna for Wireless Communication Networks. IEEEAccess 2022, 10, 25278–25289S.

11) Liu, "Wi-Fi Energy Detection Testbed (12MTC)," 2023, gitHub repository. [Online]. Available: https://github.com/liustone99/Wi-Fi-Energy-Detection-Testbed- 12MTC

12) "Treatment episode data set: discharges (TEDS-D): concatenated, 2006 to 2009." U.S. Department of Health and Human Services, Substance Abuse and Mental Health Services Administration, Office of Applied Studies, August, 2013, DOI:10.3886/ICPSR30122.v2

13) Tang, Z.; Wu, X.; Zhan, J.; Hu, S.; Xi, Z.; Liu, Y. Compact UWB-MIMO Antenna with High Isolation and Triple Band-Notched Characteristics. IEEE Access 2019, 7, 19856–19865.

14) Chen, Z.; Zhou, W.; Hong, J. A Miniaturized MIMO Antenna with Triple Band-Notched Characteristics for UWB Applications. IEEE Access 2021, 9, 63646– 63655.

15) Abdelhamid, C.; Daghari, M.; Sakli, H.; Hamrouni, C. High Isolation with Metamaterial Improvement in A Compact UWB MIMO Multi-Antennas. In Proceedings of the 2019 16th International Multi-Conference on Systems, Signals & Devices (SSD), Istanbul, Turkey, 21–24 March 2019.

16) Khan, A.; Bashir, S.; Ghafoor, S.; Qureshi, K.K. Mutual Coupling Reduction Using Ground Stub and EBG in a Compact Wideband MIMO-Antenna. IEEE Access 2021, 9, 40972–40979. [CrossRef]

17) Zhang, S.; Pedersen, G.F. Mutual Coupling Reduction for UWB MIMO Antennas with a Wideband Neutralization Line. IEEE Antennas Wirel. Propag. Lett. 2016, 15, 166–169. [CrossRef]

18) .Wang,S.-L.; Hong, J.-S.; Wang, C.; He, J.-F. A nonplanar quad-element UWB-MIMO antenna with graphite sheet to increase the isolation. In Proceedings of the 2018 IEEE MTT-S International Wireless Symposium (IWS), Chengdu, China, 6–10 May 2018; pp. 1–3

19) Khan, M.S.; Capobianco, A.-D.; Asif, S.M.; Anagnostou, D.E.; Shubair, R.M.; Braaten, B.D. A Compact CSRR-Enabled UWB Diversity Antenna. IEEE Antennas Wirel. Propag. Lett. 2017, 16, 808–812.

20) Luo, C.-M.; Hong, J.-S.; Zhong, L.-L. Isolation enhancement of a very compact UWB-MIMO slot antenna with two defective ground structures. IEEE Antennas Wirel. Propag. Lett. 2015, 14, 1766–1769.

21) K. Venu Gopal and Y. Srinivasa Rao "UWB MIMO Antenna with Enhanced Isolation Using SRR" Int. Journal of Microwave and Optical Technology, VOL.18, NO.3, Page No:223-228, MAY 2023.

22) Anitha, R.; Sarin, V.P.; Mohanan, P.; Vasudevan, K. Enhanced isolation with defected ground structure in MIMO antenna. Electron. Lett. 2014, 50, 1784–1786.

23) Ren, J.; Hu, W.; Yin, Y.; Fan, R. Compact Printed MIMO Antenna for UWB Applications. IEEE Antennas Wirel. Propag. Lett. 2014, 13, 1517–1520.

Tianjin Daxue Xuebao (Ziran Kexue yu Gongcheng Jishu Ban)/
Journal of Tianjin University Science and Technology
ISSN (Online):0493-2137
E-Publication: Online Open Access
Vol: 57 Issue: 12:2024
DOI: 10.5281/zenodo.16525521

24) Niu, Z.; Zhang, H.; Chen, Q.; Zhong, T. Isolation Enhancement for 1 3 Closely Spaced E-Plane Patch Antenna Array Using Defect Ground Structure and Metal- Vias. IEEE Access 2019, 7, 119375–119383.

25) UlHM, A.; Slawomir, K. Ground Plane Alterations for Design of High-Isolation Compact Wideband MIMO Antenna. IEEE Access 2018, 6, 48978–48983.

26) Raheja, D.K.; Kanaujia, B.K.; Kumar, S. Compact four-port MIMO antenna on the slotted-edge substrate with dual-band rejection characteristics. Int. J. RF Microw. Comput.-Aided Eng. 2019, 29, e21756. [CrossRef]

27) Rao, P.K.; Mishra, R. Elliptical Shape Flexible MIMO Antenna with High Isolation for Breast Cancer Detection Application. IETE J. Res. 2020, 69, 325–333. [CrossRef]

28) Gómez-Villanueva, R.; Jardón-Aguilar, H. Compact UWB Uniplanar Four-Port MIMO Antenna Array with Rejecting Band. IEEE Antennas Wirel. Propag. Lett. 2019, 18, 2543–2547. [CrossRef]

29) Keerthana, G.; Naidu, P.V.; Priyanka, K.; Sumanji, L.; Saiharanadh, A.; Maheshbabu, D.; Kumar, A.; Priyanka, V. High Isolation Compact Four Port MIMO Antenna with Slotted Ground for UWB Applications. In Proceedings of the 2021 Photonics & Electromagnetics Research Symposium (PIERS), Hangzhou, China, 22 November 2021; pp. 1441–1448. [CrossRef]

30) Desai, A.; Kulkarni, J.; Kamruzzaman, M.M.; Hubálovský, Š.; Hsu, H.-T.; Ibrahim, A.A. Interconnected CPW Fed Flexible 4-Port MIMOAntennafor UWB,X,andKuBandApplications. IEEE Access 2022, 10, 57641–57654. [CrossRef]

31) Mathur, R.; Dwari, S. A compact 4-port UWB-MIMO/diversity antenna for WPAN application. In Proceedings of the 2018 3rd International Conference on Microwave and Photonics (ICMAP), Dhanbad, India, 9–11 February 2018; pp. 1–2.